ЖЭТФ, 2005, том 128, вып. 1 (7), стр. 193–200

SURFACE GRAVITY WAVES IN DEEP FLUID AT VERTICAL SHEAR FLOWS

G. Gogoberidze**, L. Samushia, G. D. Chagelishvili, J. G. Lominadze

Center for Plasma Astrophysics, Abastumani Astrophysical Observatory
0160, Tbilisi, Georgia

W. Horton

Institute for Fusion Studies, The University of Texas at Austin
Austin, Texas 78712

Submitted 28 October 2004

Special features of surface gravity waves in a deep fluid flow with a constant vertical shear of velocity is studied. It is found that the mean flow velocity shear leads to a nontrivial modification of the dispersive characteristics of surface gravity wave modes. Moreover, the shear induces generation of surface gravity waves by internal vortex mode perturbations. The performed analytical and numerical study show that surface gravity waves are effectively generated by the internal perturbations at high shear rates. The generation is different for the waves propagating in the different directions. The generation of surface gravity waves propagating along the main flow considerably exceeds the generation of surface gravity waves in the opposite direction for relatively small shear rates, whereas the latter wave is generated more effectively for high shear rates. From the mathematical standpoint, the wave generation is caused by non-self-adjointness of the linear operators that describe the shear flow.

PACS: 92.10.Hm, 47.35.+i, 47.27.Pa

1. INTRODUCTION

Generation of surface gravity waves (SGW), which are the best known sea and oceanic waves, is naturally associated with winds. Momentum transfer from wind to undulating movement of the ocean, which is the basic mechanism of the generation of surface waves, is investigated since Kelvin's pioneering work [1]. Independent and inter-complementary theories of Phillips [2] and Miles [3–6] provide the basics of theoretical understanding of surface wave generation by wind. Phillips' resonant mechanism is responsible for excitation and initial rising of wave motion on an unexcited surface of the fluid; Miles' mechanism — energy transfer from wind to fluid as a consequence of the interaction between wind shear flow and surface waves — is responsible for subsequent amplification of the waves. According to Miles' mechanism, the energy source is the wind shear flows situated outside the fluid. Other ways of SGW generation have also been studied, such as the possibility of SGW generation by earthquakes [7, 8] and the theory of SGW generation by intrafluid explosions [9]. In the theories mentioned above, the sources of SGW generation are extrinsic to the fluid.

The question arises as to whether sources intrinsic for the fluid (shear flows and vortex perturbations, for example) can generate SGW.

This question becomes especially interesting in view of the impressive progress made in the understanding of spectrally stable shear flow phenomena by the hydrodynamic community in the past ten years. The early transient period for the perturbations has been shown to reveal rich and complicate behavior in smooth (without inflection point) shear flows. In particular, it has been shown that the linear dynamics of perturbations in the flows are accompanied by intense temporal energy exchange processes between the background flow and perturbations and/or between different modes of perturbations. From the mathematical standpoint, these effects are caused by the non-self adjointness of the linear operators in shear flows and are adequately

*E-mail: gogober@geo.net.ge

described in the framework of the so-called nonmodal approach (see, e.g., [10–12]). The nonmodal approach involues a change of independent variables from the laboratory frame to a moving frame and the study of temporal evolution of spatial Fourier harmonics (SFHs) of perturbations without any spectral expansion in time.

We examine the linear dynamics of surface waves and internal perturbations in deep fluid in the absence of wind and in the presence of the fluid flow with a vertical shear of velocity. Dispersive characteristics of shear-modified SGWs and the linear mechanism of the generation of surface waves in deep fluid by internal perturbations are studied in detail in the framework of the nonmodal approach.

The paper is organized as follows: the mathematical formalism is presented in Sec. 2. Shear-modified SGWs and their generation are analyzed in Sec. 3. Applications of the obtained results to the concrete physical problems are discussed in Sec. 4. Conclusions are given in Sec. 5.

2. MATHEMATICAL FORMALISM

We consider deep fluid with the flat outer surface at $z = 0$ and a constant shear flow $\mathbf{U}_0 = (Az, 0, 0)$ for $z < 0$. The shear parameter A is considered positive for simplicity. The gravitational field is considered uniform, $\mathbf{g} = (0, 0, -g)$. Generally, four modes of perturbation (SGW, internal gravity waves, sound waves, and vortex mode) can exist in the system. To reduce the mathematical complications as much as possible but still keep the basic physics of our analysis, we consider fluid to be incompressible (neglecting sound waves) and disregard the stratification effects (assuming that the frequency of internal gravity waves is much less than the frequency of SGWs, i.e., considering internal gravity waves as aperiodic/vortex mode perturbations). We also ignore the effects of viscosity in what follows. After these simplifications, we keep just two modes of perturbation, SGW and the vortex mode, and write the differential equations for the linear dynamics of perturbations of velocity ($\mathbf{u}'$) and normalized pressure ($p' = p/\rho_0$) as

$$\frac{\partial u'_x}{\partial x} + \frac{\partial u'_y}{\partial y} + \frac{\partial u'_z}{\partial z} = 0, \tag{1}$$

$$\frac{\partial u'_x}{\partial t} + Az\frac{\partial u'_x}{\partial x} + Au'_z = -\frac{\partial p'}{\partial x}, \tag{2}$$

$$\frac{\partial u'_y}{\partial t} + Az\frac{\partial u'_y}{\partial x} = -\frac{\partial p'}{\partial y}, \tag{3}$$

$$\frac{\partial u'_z}{\partial t} + Az\frac{\partial u'_z}{\partial x} = -\frac{\partial p'}{\partial z}, \tag{4}$$

with the boundary condition on the surface $z = 0$:

$$\left(\frac{\partial p'}{\partial t} - gu'_z\right)\Big|_{z=0} = 0. \tag{5}$$

We use the standard technique of the nonmodal approach [10]: introduction of comoving variables ($x' = x + Azt$, $y' = y$, $z' = z$, $t' = t$) allows us to transform the spatial inhomogeneity presented in Eqs. (1)–(5) into a temporal one. Then, after the Fourier transformation with respect to x' and y',

$$\mathbf{u}'(\mathbf{r}, t) = \frac{1}{4\pi^2}\int \mathbf{u}(k_x, k_y, z', t) \times \times \exp\left[i(k_x x' + k_y y')\right] dk_x dk_y, \tag{6}$$

the dynamic equations are reduced to

$$ik_x u_x + ik_y u_y + \left(\frac{\partial}{\partial z'} - iAt'k_x\right) u_z = 0, \tag{7}$$

$$\frac{\partial u_x}{\partial t'} + Au_z = -ik_x p, \tag{8}$$

$$\frac{\partial u_y}{\partial t'} = -ik_y p, \tag{9}$$

$$\frac{\partial u_z}{\partial t'} = -\left(\frac{\partial}{\partial z'} - iAt'k_x\right) p, \tag{10}$$

$$\left(\frac{\partial p}{\partial t'} - gu_z\right)\Big|_{z'=0} = 0. \tag{11}$$

Hereafter, the primes of the z' and t' variables are omitted.

From this set, we readily obtain the equation for the perturbation of the vertical component of velocity,

$$\frac{\partial}{\partial t}\left(\left[\widetilde{k}^2 - \left(\frac{\partial}{\partial z} - iAtk_x\right)^2\right] u_z\right) = 0, \tag{12}$$

where $\widetilde{k} = \sqrt{k_x^2 + k_y^2}$.

All other perturbed quantities (u_x, u_y, and p) can be readily expressed through u_z by combining Eqs. (7)–(10); e.g., for p, we have

$$p = -\frac{1}{\widetilde{k}^2}\left(\frac{\partial}{\partial t}\left[\left(\frac{\partial}{\partial z} - iAtk_x\right) u_z\right] - iAk_x u_z\right). \tag{13}$$

Integration of Eq. (12) with respect to time yields

$$\left[\widetilde{k}^2 - \left(\frac{\partial}{\partial z} - iAtk_x\right)^2\right] u_z(k_x, k_y, z, t) = = F(k_x, k_y, z), \quad (14)$$

where $F(k_x, k_y, z)$ is the constant (in time) of integration and defines the internal vortex mode perturbation in the flow: $F(k_x, k_y, z) = 0$ relates to the case where the internal perturbation is absent.

The Fourier transformation with respect to z,

$$\begin{bmatrix} u_z(k_x, k_y, z, t) \\ F(k_x, k_y, z) \end{bmatrix} = = \frac{1}{2\pi} \int\limits_{-\infty}^{\infty} \begin{bmatrix} u_z(k_x, k_y, k_z, t) \\ \widetilde{F}(k_x, k_y, k_z) \end{bmatrix} e^{ik_z z} dk_z, \quad (15)$$

reduces Eq. (14) to

$$k^2(t) u_z(k_x, k_y, k_z, t) = \widetilde{F}(k_x, k_y, k_z) + + 4i\pi\widetilde{k} C(k_x, k_y, t), \quad (16)$$

where

$$C \equiv \frac{1}{4i\pi\widetilde{k}} \times \times \left[\left(\frac{d}{dz} - 2iAtk_x - ik_z\right) u_z(k_x, k_y, z, t)\right]\Big|_{z=0}. \quad (17)$$

Defining $u_z(k_x, k_y, k_z, t)$ from Eq. (16), making the inverse Fourier transformation atom with respect to k_z, taking the boundary condition $|u_z| < \infty$ at $z = -\infty$ into account, and recalling that $C(k_z, k_y, t)$ is independent of z, we obtain

$$u_z(k_x, k_y, z, t) = \frac{1}{2\pi} \int\limits_{-\infty}^{\infty} \frac{\widetilde{F}(k_x, k_y, k_z)}{k^2(t)} \exp(ik_z z)\, dk_z + + C(k_x, k_y, t) \exp[(\widetilde{k} + iAtk_x)z], \quad (18)$$

where $k^2(t) = \widetilde{k}^2 + k_z^2(t)$ and $k_z(t) \equiv k_z - Atk_x$.

The first term in Eq. (18) is related to the vortex mode perturbation [11, 13], whereas the second term, which is exponentially decreasing with the depth, is related to the SFHs of shear modified surface waves.

Substituting Eq. (18) in Eq. (13) and using boundary condition, Eq. (11), we obtain

$$\frac{d^2C}{dt^2} + \frac{iAk_x}{\widetilde{k}} \frac{dC}{dt} + \widetilde{k}gC = I(k_x, k_y, t), \quad (19)$$

where

$$I(k_x, k_y, t) \equiv \equiv \int\limits_{-\infty}^{\infty} \left[8iA^2 k_x^2 \widetilde{k} \frac{k_z(t)}{k^6(t)} - \frac{\widetilde{k}g}{k^2(t)}\right] \widetilde{F}(\mathbf{k})\, dk_z. \quad (20)$$

Generally, Eqs. (19)–(20) describe the dynamics of surface wave SFHs in the presence of the internal vortical source: the term $I(k_x, k_y, t)$ is the result of an interplay of the mean flow shear and the internal vortical perturbations and couples the latter perturbation to the surface one. Hence, there is no coupling between these perturbations in the absence of the shear. Indeed, if there are no surface perturbations initially $[u_z(k_x, k_y, z = 0, t = 0) = 0]$, then we readily obtain from Eqs. (16) and (20) that $I(k_x, k_y, t) \sim u_z(k_x, k_y, z = 0, t = 0)$ at $A = 0$, i.e., $I(k_x, k_y, t) \equiv 0$. Thus, if there is no the source in a shearless flow initially, it does not appear afterward.

3. SGWs AND THEIR GENERATION IN SHEAR FLOW

We can see from Eqs. (19) and (20) that there are two main effects of the shear: first, the second term in the left-hand side of Eq. (19) indicates that the velocity shear affects the frequencies of SGWs. Second, the source term $I(k_x, k_y, t)$ caused by the internal perturbations couples the internal and surface perturbations and results in the emergence/generation of SGW in the flow. Our further attempts are focused on the study of these effects.

A. Shear modified SGWs

In this subsection, we study shear-induced modifications of the properties of SGWs. For this, we assume that there were no vortex mode perturbations initially, $\widetilde{F}(k_x, k_y, k_z) = 0$. Consequently, $I(k_x, k_y, t) = 0$ [see Eqs. (20)], and Eq. (19) reduces to a homogeneous one, with the solution

$$C_h(k_x, k_y, t) = C_1(k_x, k_y) \times \times \exp(-i\Omega_1 t) + C_2(k_x, k_y) \exp(-i\Omega_2 t), \quad (21)$$

where $C_{1,2}(k_x, k_y)$ are determined by the initial conditions and

$$\Omega_{1,2} = \pm\sqrt{\widetilde{k}g + \frac{A^2k_x^2}{4\widetilde{k}^2}} - \frac{Ak_x}{2\widetilde{k}} = = \sqrt{\widetilde{k}g}\left(\pm\sqrt{1 + S^2\frac{k_x^2}{\widetilde{k}^2}} - S\frac{k_x}{\widetilde{k}}\right) \quad (22)$$

represents shear-modified frequencies of SFH of a SGW propagating in the opposite directions and $S \equiv A/(4\widetilde{k}g)^{1/2}$ is the dimensionless shear rate. This equation shows that in contrast to acoustic and magnetohydrodynamic wave modes [14–16], the presence of

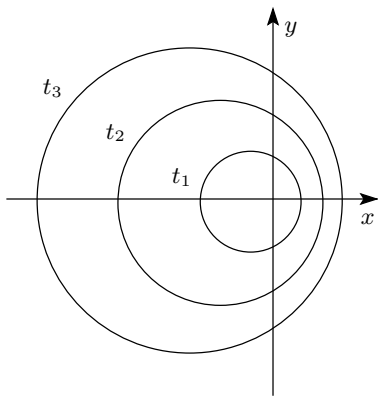

Fig. 1. Shear-induced anisotropy of SGW propagation: the leading wave crest at three different time instants t_1, t_2, t_3, with $t_2 = 2t_1$, $t_3 = 3t_1$, which are circular but not concentric. A point source of the SGW is located at $x = y = 0$

the shear does not lead to the time variability of the frequency. However, velocity shear leads to a nontrivial modification of the frequencies and, consequently, phase velocities of SFH [17, 18]. Indeed, for the value of the phase velocity, Eq. (22) gives

$$V_{ph}(S,\phi) = \sqrt{\frac{g}{\widetilde{k}}}\left(\sqrt{1+S^2\cos^2\phi} - S\cos\phi\right), \quad (23)$$

where $\phi \equiv \arccos(k_x/\widetilde{k})$.

The phase velocity is isotropic in the shearless limit ($S = 0$) and depends on ϕ in the shear flow. The anisotropy increases with the shear rate. The value of the phase velocity is minimal at $\phi = 0$, $V_{ph}^{\min} = \sqrt{g/\widetilde{k}}(\sqrt{1+S^2} - S)$, and is maximal at $\phi = \pi$, $V_{ph}^{\max} = \sqrt{g/\widetilde{k}}(\sqrt{1+S^2} + S)$. We suppose that a SGW is emitted by a point source situated on the surface at $x = y = 0$. From Eq. (23), it then follows that the propagation of the leading wave crest is described by

$$r(S,\phi,t) = V_{ph}(S,\phi)t = \\ = \sqrt{\frac{g}{\widetilde{k}}}\left(\sqrt{1+S^2\cos^2\phi} - S\cos\phi\right)t. \quad (24)$$

Figure 1 shows the leading wave crest of the SGW for three different time instants t_1, t_2, t_3, with $t_2 = 2t_1$, $t_3 = 3t_1$, which are circular but not concentric.

B. Generation of SGWs by internal vortices

We first analyze the source term $I(k_x, k_y, t)$, which is determined by $\widetilde{F}(k_x, k_y, k_z)$. We assume that $\widetilde{F}(k_x, k_y, k_z)$ is a localized function in the wavenumber space, with the center of localization at $\mathbf{k}_0 = (k_{x0}, k_{y0}, k_{z0})$. We note that the first factor in the integrand in Eq. (20) reaches its maximum when $k_z - Ak_x t = 0$. Consequently, the maximum of the integral is in the vicinity of the time instant $t = t_* \equiv k_{z0}/(Ak_{x0})$. Equation (20) implies that generally, $I(k_x, k_y, t)$ tends to zero in both limits $t \to \pm\infty$. Actually, there exists some time interval $2\Delta t$ around t_* where the source term differs from zero. The value of Δt depends on the degree of localization of the internal perturbation, i.e., of $\widetilde{F}(k_x, k_y, k_z)$, in the wavenumber space. (The source localization is demonstrated below in a specific example.) Thus, in the case of a localized source, the coupling between surface (gravity wave) and internal (vortex mode) perturbations takes place in some time interval $2\Delta t$ around t_*, and these perturbations can be considered separately at $|t - t_*| > \Delta t$.

The general solution of the inhomogeneous equation, Eq. (19), is the sum of the general solution of the corresponding homogenous equation and a partial solution of the equation

$$C(k_x, k_y, t) = C_h(k_x, k_y, t) + C_i(k_x, k_y, t). \quad (25)$$

The general solution $C_h(k_x, k_y, t)$ is given by Eq. (21), whereas a partial solution of Eq. (19) is

$$C_i = \frac{1}{2\Omega_0}\exp(-i\Omega_1 t)\int_{t_0}^{t} I(k_x, k_y, t')\exp(i\Omega_1 t')\,dt' - \\ - \frac{1}{2\Omega_0}\exp(-i\Omega_2 t)\times \\ \times \int_{t_0}^{t} I(k_x, k_y, t')\exp(i\Omega_2 t')\,dt', \quad (26)$$

where

$$\Omega_0 = \sqrt{\widetilde{k}g + \frac{A^2k_x^2}{4\widetilde{k}^2}} = \sqrt{\widetilde{k}g}\sqrt{1 + S^2\frac{k_x^2}{\widetilde{k}^2}}. \quad (27)$$

We assume that the coupling between the surface and internal modes can be neglected at the initial time instant t_0, i.e., $t_0 < t_* - \Delta t$. After passing through the coupling time interval, for any $t > t_f = t_* + \Delta t$, the modes become independent again. However, during the time interval $[t_0, t_f]$, internal vortices generate SGWs with frequencies Ω_1 and Ω_2 [see Eq. (22)]. As follows from Eqs. (21), (25), and (26), if there are no SGWs ($C_{1,2} = 0$) initially, then the generated SFH amplitudes ($Q_{1,2}$) are

$$Q_1(k_x,k_y)=\frac{1}{2\Omega_0}\times \times\left|\int\limits_{t_0}^{t_f} I(k_x,k_y,t')\exp\left(i\Omega_1 t'\right)dt'\right|, \quad (28)$$

$$Q_2(k_x,k_y)=\frac{1}{2\Omega_0}\times \times\left|\int\limits_{t_0}^{t_f} I(k_x,k_y,t')\exp\left(i\Omega_2 t'\right)dt'\right|. \quad (29)$$

We can replace the integration limits by $\pm\infty$. After integration over time, this yields

$$Q_{1,2}=\frac{\pi k_x}{\widetilde{k}^3}\left(\frac{A}{2\Omega_0}\mp\frac{k_x}{\widetilde{k}}\right)\exp\left[-\frac{(\Omega_0\mp A/2)\widetilde{k}}{Ak_x}\right]\times \times\int\widetilde{F}(k_x,k_y,k_z)\exp\left(-i\frac{(\Omega_0\mp A/2)k_z}{Ak_x}\right)dk_z= =\frac{2\pi^2 k_x}{\widetilde{k}^3}\left(\frac{A}{2\Omega_0}\mp\frac{k_x}{\widetilde{k}}\right)\exp\left[-\frac{(\Omega_0\mp A/2)\widetilde{k}}{Ak_x}\right]\times \times F\left(k_x,k_y,-\frac{\Omega_0\mp A/2}{Ak_x}\right). \quad (30)$$

We note that the last factors in Eq. (30) are proportional to the vorticity of the initial perturbations at $z_{1,2}=-(\Omega_0\mp A/2)/(Ak_x)$ respectively. The second factors indicate that at small shear rates ($S\equiv A/\sqrt{4\widetilde{k}g}\ll 1$), the amplitudes of the generated SGWs are exponentially small with respect to the large parameter $1/S$. Equation (30) also indicates that for a fixed k_x, the generation is most efficient in the two-dimensional case ($k_y=0$).

We now describe the dynamic picture for a specific example, where a pure internal vortex-mode perturbation (without any admixture of surface waves) is imposed in the flow initially. For simplicity, we consider the two-dimensional problem, where $\partial/\partial y=0$. The vertical velocity of the imposed perturbation is given by

$$u_z(x,z,t_0)=z^3\eta(-z)\times \times\exp\left(-\frac{[(z+z_0)\cos\phi+x\sin\phi]^2}{L_1^2}\right)\times \times\exp\left(-\frac{[(z+z_0)\sin\phi-x\cos\phi]^2}{L_2^2}\right), \quad (31)$$

where $\eta(z)$ is Heaviside function, $(0,-z_0)$ is the center of the localization, $L_{1,2}$ characterize the vertical and horizontal scales respectively, and ϕ is the slope of the perturbation.

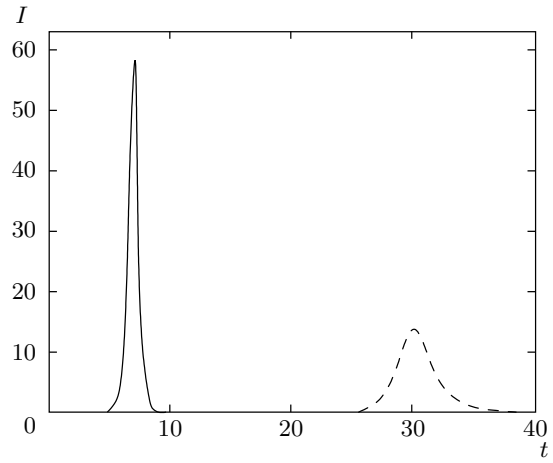

Fig. 2. $I(k_x,k_y,t)$ vs time at $S=0.32$ (solid line) and $S=0.08$ (dashed line), $k_x=1$, $L_1=1$, $L_2=7$, $z_0=2$ and $\phi=\pi/18$

Numerical solution of the problem was performed as follows: Fourier transformation of Eq. (31) with respect to the x variable allows us to determine $F(k_x,z)$ through Eq. (14). Another Fourier transformation with respect to z yields $\widetilde{F}(k_x,k_z)$. Then the source function $I(k_x,t)$ is found by Eq. (20). Thus, the solution of the problem for a fixed k_x reduces to the numerical solution of the inhomogeneous equation, Eq. (19), with the known $I(k_x,t)$.

The dependence of the source function $I(k_x,t)$ on t at $L_1=1$, $L_2=7$, $\phi=\pi/18$, $k_x=1$, and $z_0=2$ for two different values of the shear rate $S=0.08$ (dashed line) and $S=0.32$ (solid line) is presented in Fig. 2. As was mentioned above, the source term is a localized function and considerably differs from zero only in the interval $t\in(20,40)$ for $S=0.08$ and $t\in(5,10)$ for $S=0.32$.

To analyze the wave generation efficiency, it is useful to introduce the generation coefficients that characterize the ratio of the generated wave energy density and the maximum energy density of the initial vortex mode perturbations for a fixed value of k_x. Taking into account that the maximum energy density of the vortex mode perturbations is

$$E_v=\frac{1}{2k_x^4}\int\limits_{-\infty}^{\infty}|F(k_x,z)|^2dz \quad (32)$$

and the energy density of the generated waves is

$$E_{w1,2}=\frac{1}{k_x}Q_{1,2}^2(k_x), \quad (33)$$

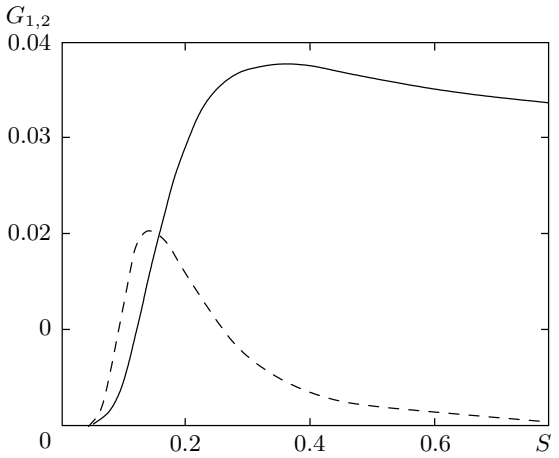

Fig. 3. The generation coefficients G_1 (dashed line) and G_2 (solid line) vs. the shear rate S at $k_x = 1$, $L_1 = 1$, $L_2 = 7$, $z_0 = 2$, and $\phi = \pi/18$

we define the dimensionless generation coefficients as:

$$G_{1,2} = Q_{1,2}(k_x) \left(\frac{2k_x^3}{\int\limits_{-\infty}^{\infty} |F(k_x, z)|^2 dz} \right)^{1/2} . \qquad (34)$$

Figure 3 represents the generation coefficients G_1 (dashed line) and G_2 (solid line) vs the shear rate S at $L_1 = 1$, $L_2 = 7$, $\phi = \pi/18$, $k_x = 1$, and $z_0 = 2$. As can be seen, at small values of the shear rate, generation of SGW with the frequency Ω_1 (i.e., propagating along the x axis) considerably exceeds the generation of SGW with the frequency Ω_2 (i.e., propagating against the x axis), whereas the latter wave is generated more efficiently at $S > 0.15$.

The wave generation is well traced in Figs. 4 and 5, where the temporal evolution of the vertical component of velocity perturbation at the surface obtained by numerical solution of Eqs. (19), (20) is presented for $S = 0.32$ and $S = 0.08$ respectively. The other parameters are the same as in Fig. 2. A purely internal vortex mode perturbation is imposed in the equations initially. The generation occurs in the time interval where $I(k_z, t)$ noticeably differs from zero. Afterwards, just (two) waves with different frequencies and amplitudes exist. At $S = 0.32$, presented in Fig. 4, the generation occurs in the time interval $t \in (5, 10)$. Besides, the SGW propagating against the x axis is mainly generated. In contrast to this, at $S = 0.08$, presented in Fig. 5, the generation of SGW propagating along the x axis dominates. These numerical results are in agreement with the analytical ones (see Eq. (30) and Fig. 3).

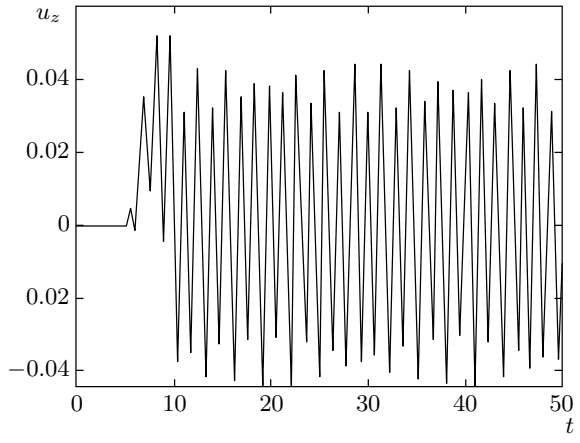

Fig. 4. $u_z(k_x, t)$ vs. time at $S = 0.32$, $k_x = 1$, $L_1 = 1$, $L_2 = 7$, $z_0 = 2$, and $\phi = \pi/18$

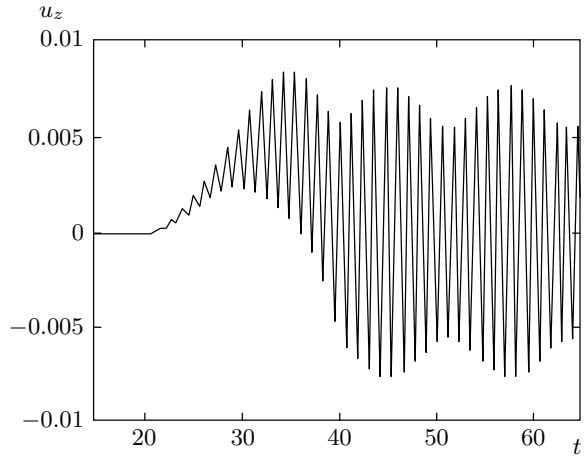

Fig. 5. $u_z(k_x, t)$ vs. time at $S = 0.08$, $k_x = 1$, $L_1 = 1$, $L_2 = 7$, $z_0 = 2$, and $\phi = \pi/18$

4. DISCUSSION

In the previous sections, a simplified model was considered that allowed us to simplify the mathematical description and study shear-induced effects in a «pure» form. For instance, the influence of the viscosity was ignored and the density ratio ρ_a/ρ_0 of the fluids above and below the surface $z = 0$ was assumed to be zero. The last assumption allows us to ignore all the dynamical processes in the upper fluid. On the other hand, it is well known that in the case of ocean waves, the

wind is the most important and powerful source of the waves. In this section, we discuss possible applications of the studied linear effects to the concrete physical situations.

A. Ocean waves

It is well known [2–6] that the wind is the main source of ocean SGWs. In the context of future discussion, the papers of Chalikov's group [19, 20] should also be noted, where the influence of small-scale turbulence in the air on the wave growth was studied in detail. At present, there exists a well-developed theory of both SGW generation and nonlinear evolution that is mainly confirmed by experiments as well as numerical simulations (see, e.g., [21] for a recent review). After development of a wind-driven instability, nonlinear 4-wave resonant interactions transfer the wave energy to smaller scales. The existing theory predicts that for relatively small frequencies, the Zakharov–Philonenko [22] spectrum $E(\omega) \propto \omega^{-4}$ of SGW fluctuations (sometimes called Toba's spectrum) should be observed (in this context, see also [23]), whereas for relatively high wave numbers, nonlinearity becomes strong and the Phillips spectrum $E(\omega) \sim \omega^{-5}$ of the wave turbulence should develop. The existing observations confirm these predictions and provide that in the range $\omega_p/3 < \omega < 3\omega_p$, where ω_p is the peak frequency, the Zakharov–Philonenko spectrum is usually observed. For $\omega > 3\omega_p$, the spectrum becomes very close to the Phillips one [21]. The properties of the wave spectrum in the very short wavelength region, as well as dynamics of dissipation of SGW turbulent fluctuations, are much less clear [24].

In the case of ocean waves, the presented linear mechanism of SGW generation can an important contribution to the balance of small-scale SGW fluctuations. Indeed, a characteristic length scale of the turbulence is much smaller at the ocean surface than in the air. Namely, the characteristic length and velocity scales are $u_* \sim 1$ cm/s and $l \sim 1$ cm respectively [25]. On the other hand, in the presence of the wind, the strong velocity shear $A \sim 10\ \mathrm{s}^{-1}$ is present in the so-called «buffer layer» [26] of the water, with the thickness $l_1 \sim (20-100)l_0$, where $l_0 \approx \nu/u_*$ is the dissipation length scale and ν is the kinematic viscosity of water. Simple estimates yield $l_1 \sim$ (0.5–1) cm. The linear mechanism presented implies that vortical perturbations generate SGWs with the same length scale. Therefore, in the case of ocean waves, internal vortex-mode perturbations should effectively generate small-scale SGWs, with the wavelength just above the capillary length scale $\lambda_c = 0.39$ cm [27]. In this context, the study of the influence of capillary effects on the processes discussed above seems to be interesting. Analysis of this problem will be presented elsewhere.

B. Interfacial gravity waves

In the analysis in Secs. 2 and 3, the density ratio ρ_a/ρ_0 of the fluids above and below the surface $z = 0$ was assumed to be zero. The obtained results can be readily generalized to the case of interfacial GWs. If the densities of the upper and lower fluids are ρ_1 and ρ_2 and the shear rates are A_1 and A_2 respectively, then the shear-modified dispersion of interfacial GWs is given by the same expression (22) with g and A replaced by g_* and A_*, where

$$g_* = g\frac{\rho_2 - \rho_1}{\rho_2 + \rho_1}, \quad A_* = \frac{A_2\rho_2 - A_1\rho_1}{\rho_2 + \rho_1}. \tag{35}$$

This equation implies that the influence of shear on both the wave dispersion and the coupling with internal vortex perturbations, which is determined by the dimensionless parameter

$$S_* \equiv \frac{A_*}{\sqrt{4\tilde{k}g_*}} = S_2\frac{1 - \rho_1 A_1/\rho_2 A_2}{\sqrt{1 - \rho_1^2/\rho_2^2}}, \tag{36}$$

is much more notable when the fluids have comparable densities if $\rho_1 A_1$ is not very close to $\rho_2 A_2$. Therefore, the described shear-induced effects should usually have much stronger effect on the dynamics of interfacial waves than on ocean waves.

5. SUMMARY

We summarize the main features of the linear dynamics of surface gravity waves in a simplified deep fluid (at $z < 0$) flow with vertical shear of the mean velocity $\mathbf{U}_0 = (Az, 0, 0)$. The simplification lies in neglecting the fluid compressibility and stratification, in other words, in the consideration of the system containing just two modes of perturbation: the surface gravity wave mode and the internal vortex mode. Special features of SGW in the system are as follows.

The mean flow velocity shear causes a nontrivial modification of the frequencies and phase velocities of SGWs. The frequencies are defined by Eq. (22). The phase velocity becomes anisotropic (see Eq. (23) and Fig. 1): its value is minimal for SFH propagating along the x axis $[V_{ph}^{min} = \sqrt{g/\tilde{k}}(\sqrt{1+S^2} - S)]$ and maximal for SFH propagating against the x axis $[V_{ph}^{max} = \sqrt{g/\tilde{k}}(\sqrt{1+S^2} + S)]$.

The mean flow velocity shear leads to the appearance of an intrinsic (to the fluid) source of SGW generation via coupling the wave to the internal vortex-mode perturbations; the coupling results in the emergence/generation of SGWs by internal vortex-mode perturbations at $S \gtrsim 0.05$. The generation is different for the waves propagating in the different directions (see Eq. 30). The generation of SGW with the frequency Ω_1 considerably exceeds the generation of SGW with the frequency Ω_2 for relatively small shear rates S, whereas the latter wave is generated more effectively for high shear rates ($S > 0.15$).

This research is supported by the ISTC grant G 553. The work was supported in part by the Department of Energy Grant № DE-FG03-96ER-54346.

REFERENCES

1. W. Kelvin, Phylos. Mag. **42**, 368 (1871).
2. P. O. Phillips, J. Fluid. Mech. **2**, 417 (1957).
3. J. W. Miles, J. Fluid. Mech. **3**, 185 (1957).
4. J. W. Miles, J. Fluid. Mech. **6**, 585 (1959).
5. J. W. Miles, J. Fluid. Mech. **10**, 496 (1961).
6. J. W. Miles, J. Fluid. Mech. **13**, 433 (1962).
7. K. Kajiura, J. Oceanogr. Soc. Jpn. **18**, 51 (1962).
8. K. Kajiura, J. Oceanogr. Soc. Jpn. **28**, 32 (1972).
9. H. C. Kranzer and J. B. Keller, J. Appl. Phys. **30**, 398 (1959).
10. P. Goldreich and D. Lynden-Bell, Mon. Not. R. Astron. Soc. **130**, 125 (1965).
11. W. O. Criminale and P. G. Drazin, Stud. Appl. Math. **83**, 123 (1990).
12. G. D. Chagelishvili, A. D. Rogava, and D. G. Tsiklauri, Phys. Rev. E **53**, 6028 (1996).
13. S. J. Chapman, J. Fluid Mech. **451**, 35 (2002).
14. G. D. Chagelishvili, A. G. Tevzadze, G. Bodo, and S. S. Moiseev, Phys. Rev. Lett. **79**, 3178 (1997).
15. G. D. Chagelishvili, R. G. Chanishvili, J. G. Lominadze, and A. G. Tevzadze, Phys. Plasmas **4**, 259 (1997).
16. A. D. Rogava, S. Poedts, and S. M. Mahajan, Astron. Astrophys. **354**, 749 (2000).
17. A. D. D. Craik, J. Fluid Mech. **37**, 531 (1968).
18. V. I. Shrira, J. Fluid Mech. **252**, 565 (1993).
19. D. V. Chalikov, Sov. Phys. Doklady **229**, 1083 (1976).
20. D. V. Chalikov and V. K. Makin, Boundary layer Meteorol. **56**, 83 (1991).
21. P. Janssen, *The Interaction of Ocean Waves and Wind*, Cambridge Univ. Press, Cambridge (2004).
22. V. E. Zakharov and N. N. Philonenko, Sov. Phys. Doklady **11**, 881 (1967).
23. S. A. Kitaigorodskii, J. Phys. Oceanogr. **13**, 816 (1983).
24. V. E. Zakharov, Eur. J. Mech. B **18**, 327 (1999).
25. S. A. Kitaigorodskii and J. L. Lumley, J. Phys. Oceanogr. **13**, 1977 (1983).
26. P. A. Chang, U. Piomelli, and W. K. Blake, Phys. Fluids **11**, 3434 (1999).
27. L. D. Landau and E. M. Lifshits, *Hydrodynamics*, Nauka, Moscow (1988), p. 336.